RNA (2000), *6*:1468–1479. Cambridge University Press. Printed in the USA.

Suppression of eukaryotic translation termination by selected RNAs

JASON CARNES,[1]* LUDMILA FROLOVA,[2]* SHAWN ZINNEN,[3] GABRIÈLE DRUGEON,[4] MICHEL PHILLIPPE,[5] JUST JUSTESEN,[6] ANNE-LISE HAENNI,[4] LESLIE LEINWAND,[1] LEV L. KISSELEV,[2] and MICHAEL YARUS[1]

[1]Department of Molecular, Cellular, and Developmental Biology, University of Colorado, Boulder, Colorado 80309-0347, USA
[2]Engelhardt Institute of Molecular Biology, Russian Academy of Sciences, 117984 Moscow, Russia
[3]Ribozyme Pharmaceuticals, Inc., Boulder, Colorado 80301-5411, USA
[4]Institut Jacques Monod, 75251 Paris Cedex 05, France
[5]Département de Biologie Génétique du Développement, Centre National de la Recherche Scientifique Unité Propre de Recherche 41, 35043 Rennes Cedex, France
[6]Department of Molecular and Structural Biology, University of Aarhus, DK-8000 Aarhus C, Denmark

ABSTRACT

Using selection-amplification, we have isolated RNAs with affinity for translation termination factors eRF1 and eRF1•eRF3 complex. Individual RNAs not only bind, but inhibit eRF1-mediated release of a model nascent chain from eukaryotic ribosomes. There is also significant but weaker inhibition of eRF1-stimulated eRF3 GTPase and eRF3 stimulation of eRF1 release activity. These latter selected RNAs therefore hinder eRF1•eRF3 interactions. Finally, four RNA inhibitors of release suppress a UAG stop codon in mammalian extracts dependent for termination on eRF1 from several metazoan species. These RNAs are therefore new specific inhibitors for the analysis of eukaryotic termination, and potentially a new class of omnipotent termination suppressors with possible therapeutic significance.

Keywords: aptamer; human; inhibitor; release factor; stop codon

INTRODUCTION

Sense triplets are decoded on the ribosome by specific transfer RNAs via base pairing between codons in mRNA and anticodon triplets in tRNA. In contrast, nonsense (termination, stop) codons are decoded in two canonical ways. UGA can be decoded as selenocysteine by a specialized tRNA-translation factor complex (selenocysteinyl-tRNA^{Sec}: SelB) that directs Sec-tRNA^{Sec} to a unique message structure (Hüttenhofer & Bock, 1998). More frequently UGA, UAA, and UAG are decoded as stop-translation signals. A single-polypeptide release factor (RF) termed eRF1 performs this function in eukaryotes and two proteins, RF1 and RF2, do so in bacteria (reviewed in Tate et al., 1996; Buckingham et al., 1997; Nakamura & Ito, 1998).

The class-1 release factor proteins RF1, RF2, and eRF1, are distinguished by their ability to trigger peptidyl-tRNA hydrolysis, catalyzed by the ribosomal peptidyl transferase when a stop codon enters the A site. Although the nature of this hydrolytic signal remains unknown, it is clear that class-1 RF proteins strongly compete with suppressor tRNAs in vitro and in vivo (Weiss et al., 1984; Curran & Yarus, 1988; Eggertsson & Soll, 1988; Drugeon et al., 1997; Le Goff et al., 1997). They therefore probably overlap the ribosomal decoding site. As has been suggested (Cantor, 1979; Moffat & Tate, 1994; Nissen et al., 1995; Ito et al., 1996; Nakamura et al., 1996; Kisselev et al., 2000) and proven recently by crystallography (Song et al., 2000), eRF1 adopts an extended, perhaps tRNA-like overall shape. Other proteins acting at the ribosomal A site, such as elongation factor EF-G and bacterial ribosome recycling factor (RRF; Nyborg et al., 1996; Selmer et al., 1999), also emulate the tRNA shape. These structural findings support a "tRNA-analog" hypothesis (Moffat & Tate, 1994); that is, that termination codons may be decoded directly by class-1 RFs, whose similar shape allows mimicry of tRNA action. Thus RFs may contact stop codons in the decoding (A) site on the ribosome. These facts suggest that RF action would be effectively inhibited by other strongly bound RNAs.

Selected RNA ligands for RF protein(s) therefore might act as highly specific inhibitors of stop codon translation. This would be useful for biochemical dissection of the pathway for translation termination. In addition, be-

Reprint requests to: Michael Yarus, Department of Molecular, Cellular, and Developmental Biology, University of Colorado, Boulder, Colorado 80309-0347, USA; e-mail: yarus@stripe.colorado.edu.
*To be considered coequal contributors.

cause a single eRF1 protein decodes all termination codons, such RNA ligands would likely comprise a new type of omnipotent termination suppressor, increasing stop codon readthrough by interfering with the usual termination pathway. Therefore we have isolated eRF ligands using selection-amplification (for review, see Wilson & Szostak, 1999). Starting with a randomized mixture of oligoribonucleotides, repetitive selection for RNA-RF binding yielded RNAs with high affinity (termed aptamers) toward the target proteins. Some of these eRF aptamers enhance suppression of stop codons by a means highly correlated with their selected affinity for, and with their inhibitory activities against, the individual biochemical steps of termination.

RESULTS

Selection

Purified eRF1 and eRF1•eRF3 were used to purify RNA molecules that bind these human release factors. Consecutive selections for radiolabeled protein-bound RNA were used, taking two forms. Mixed cellulose ester filters retain protein, and allow nucleic acids to flow through. These filters thereby separate RNA bound to purified release factors from free RNA. Electrophoretic mobility shift assays also provide a means to separate RNA bound to protein from free RNA. In this method, protein-bound RNAs migrate more slowly than free RNA during native polyacrylamide gel electrophoresis.

RNAs binding to human eRF1 were selected using binding to an almost-complete protein, amino acids 1–415 of a total of 437. This protein is competent in all biochemical assays, including binding to the eRF3 protein (Merkulova et al., 1999). In the selection using eRF1 a significant increase in RNA bound on filters was detected at round 9 of selection. This pool of RNAs was converted to cDNA and cloned.

In the eRF1•eRF3 selection, binding was observed at round 3 of the filter selection. However, significant increases in the filter binding background (without protein) were simultaneously detected. Thus the predominant RNAs early in the eRF1•eRF3 selection mainly had affinity for the cellulose ester filters. Switching to electrophoretic gel mobility shift selection for two rounds alleviated this problem, and significant binding to eRF1•eRF3 was subsequently observed at round 9. Because the enrichment for RNA bound to release factor did not significantly change with additional cycles of selection, these pools of RNA were cloned as cDNAs and sequenced.

Aptamer sequences selected for binding to human eRF1 and eRF1•eRF3 complex are shown in Figure 1. The approximate dissociation constants (estimated as the half-dissociation points) of the majority of individual RNA aptamers from their target was found to be 110–360 nM for eRF1 aptamers, and 60–100 nM for eRF1•eRF3 aptamers. Therefore RNAs directed at the heterodimer are the tighter binding, by approximately 1 kcal/mol. Isolated aptamers were grouped into families with obvious sequence similarities for characterization.

eRF1•eRF3 aptamers were individually characterized by binding

Although eRF1 and eRF3 proteins strongly heterodimerize in vitro, occasional free monomers of eRF1 or eRF3, or even contaminating proteins, might also serve as a target during selection. Filter assays for binding were compared for eRF1•eRF3 complex, for purified eRF1 alone, and for eRF3 alone (Fig. 2) to constrain their actual binding target, and to confirm the selected specificities.

The binding characteristics of eRF1•eRF3 aptamers fell into two functionally different classes. Class I aptamers (e.g., RNA 12) bound to eRF1 in a manner almost identical to binding to eRF1•eRF3 complex, and exhibited virtually no binding to eRF3 alone. The simplest interpretation is that Class I RNAs contact mostly a region of the eRF1 protein. This notion is strongly supported by the occurrence of sequences from the eRF1•eRF3 selection that differ by only a few nucleotides from sequences recovered with eRF1 alone. For example, the RNA 12–RNA 17 Class I eRF1•eRF3 family of sequences is clearly related to the similar eRF1 RNA 28 family, and the Class I eRF1•eRF3 RNA 11 is related to the eRF1 RNA 19 (Fig. 1). These Class I RNAs therefore contact a site exposed in both free human eRF1 and in the eRF1•eRF3 heterodimer.

The recovery of such similar aptamers from independent selections conducted with purified eRF1 from different and independent sources also makes it highly probable that these RNAs are directed at prominent regions on the *bona fide* human eRF1 protein.

Class II aptamers (e.g., RNA 27) bound to both eRF1 alone and eRF3 alone, but with notably weaker affinity than when binding eRF1•eRF3 complex. Class II RNAs therefore probably contact features exposed on both eRF1 and eRF3 proteins of the human release factor heterodimer. Complementary affinities to separately purified eRF1 and eRF3 also make it very likely that Class II RNAs have been selected for affinity to *bona fide* release factor proteins, rather than contaminants. As might be expected, Class II RNAs, which appear to be directed to distinct protein sites, are unlike sequences recovered in the eRF1 selection (Figs. 1 and 3).

Secondary structure analysis of aptamers

Apparent secondary structures of aptamers to be tested for release factor activity (below) were determined by probing the susceptibility of individual phosphodiester bonds with Pb^{2+} and S1 nuclease. Both reagents selectively hydrolyze RNA at flexible or unstructured re-

A. eRF1

Isolate	Inhibit release?	Initially randomized positions
19, 20	yes	UGGGCUGAUGGACAACCCCGAUCUCCGUGUU
2, 5, 7, 8, 12, 47	yes	AUGCAAG.CCGUACGCCGGGAAACUGGCGC.C
6, 18, 30, **34**	yes	CAUCA...CCGUACGCCGGGCAACUGGCGC.UGA
14, 31, 33, 37, 39, 40		GCAAGCAAUGAGCCCAGCUC...CACCAGGA
15, 36		GCAAGCAAUGAGCCCAGCUC...CACCAGGG
9, 13, 23, 29		GCAAGCAAUGAGCCCAGCUC.UGCACCAGGA
1, **28**, 38	yes	GUA.GCCAUAGUGC. . . . . .GAAGCAGAGC.CGUUUCA
25, 45		GUA.UCCUUCAGUGA . . . . .GAAGCAGAGC.AUUUAA
24		GUA.CCUCACAAUCG . . . . .GAAGCAGAGC.CACCCU
46		GUA.CCUCACUGG . . . . . .GAAGCAGAGC.GGAUGAGC
17		GUA.AUGCUAGAGAGCAU. . . .GAAGCAGAGC.GCA
27		GUA.CCAUAGUGC . . . . . .GAAGCAGAGC.CGUUUCA
26, 43		GUA.ACCACUGUG . . . . . .CAAGCAGAGC.CUGCAGC
4		GUA.CCUUUAUGG . . . . . .GAAGCAGGGC.GUGGAGG
16		GUA.CGCG. . . . . .GGAGCAGAGC.CGUUCAUCCAGG
3		GUA.CACGUG. . . . . .GAAGCAGGGC.GCUCCUUAGGAU
11		GUA.UCCUUUAGUGA . . . . .GAAGCAGUGC.GGCUUA
10		GUA.UCCAGUAAGUGAGAACGCAG.GAAGCGCAGGC

B. eRF1•eRF3

Isolate	Class	Inhibit release?	Initially randomized positions
11	I	No	UGGGCUGAUGGACAACCCCGAUCUCCGUGU
34, 35, **12**, B	I	Yes	GUA.CCUGAAAA..UGG.GAAGCAGAGC.GAGCCU
6, 9, 39	I		GUA.CCUGCAA...UGG GAAGCAGAGC.GGGCGGA
17	I	Yes	GUA.GCCAAAAG..UGC.GAAGCAGAGC.UAGUAA
28			GUA.GCCAAAAG..UGC.GAAGCAGAGC.GAGUAG
13			GUA.CCUGAAAAA.UGG.GAAGCAGAGC.GAGCUU
D			GUA.CCUGAAAA..UGG.GAAGCAGAGC.G
16			GUA.CCGCCUACGCUGG.GAAGCAGAGC.UAUA
C	II	No	. . . . .GGAUCCG.UAGAAAGGCCACCAGUGCUACAG
G	II	No	. . . . .GGAUCCG.UGAUACAUUUGCUUUAAACUAAC
27	II	No	. . . A .GGAUCCG.CUUACGAAAGGCCAACAACGAA
23			. . .CA .GGAUCCG.GGUUCAGAAACUGUCGUCUGU
1	II	No	. . .CA .GGAUCCG.UGACGGAGGCAAACUAAGACU
26	II		. . GCA .GGAUCCG.CUUUUAACCCCGGACUAUUA
37	II	No	GCUUCGGGU.GAGUCG.UAUUAAGCCCCGG
41			GUUCAAA..GGAUCCG.GGUCACCUGACAUUAU

FIGURE 1. **A**: Sequences selected for binding to human eRF1 alone. **B**: Sequences selected for binding to human eRF1•eRF3 complex. The sequences correspond only to the initially randomized nucleotides. Full-length RNA contains a 5′ fixed sequence, GGGAGCUCAGAAUAAACGCUCAA, as well as a 3′ fixed sequence, UUCGACAUGAGACACGGAUCC UGC. Dots are inserted in sequences to make alignment of similar sequences (motifs) more evident; there are no nucleotides at dotted positions. Isolates with bold numbers are those characterized biochemically. Note that eRF1 and eRF1•eRF3 RNAs sometimes have the same isolate numbers, but there is no overlap in the numbers chosen for characterization, thus no ambiguity about the sequences named in the text.

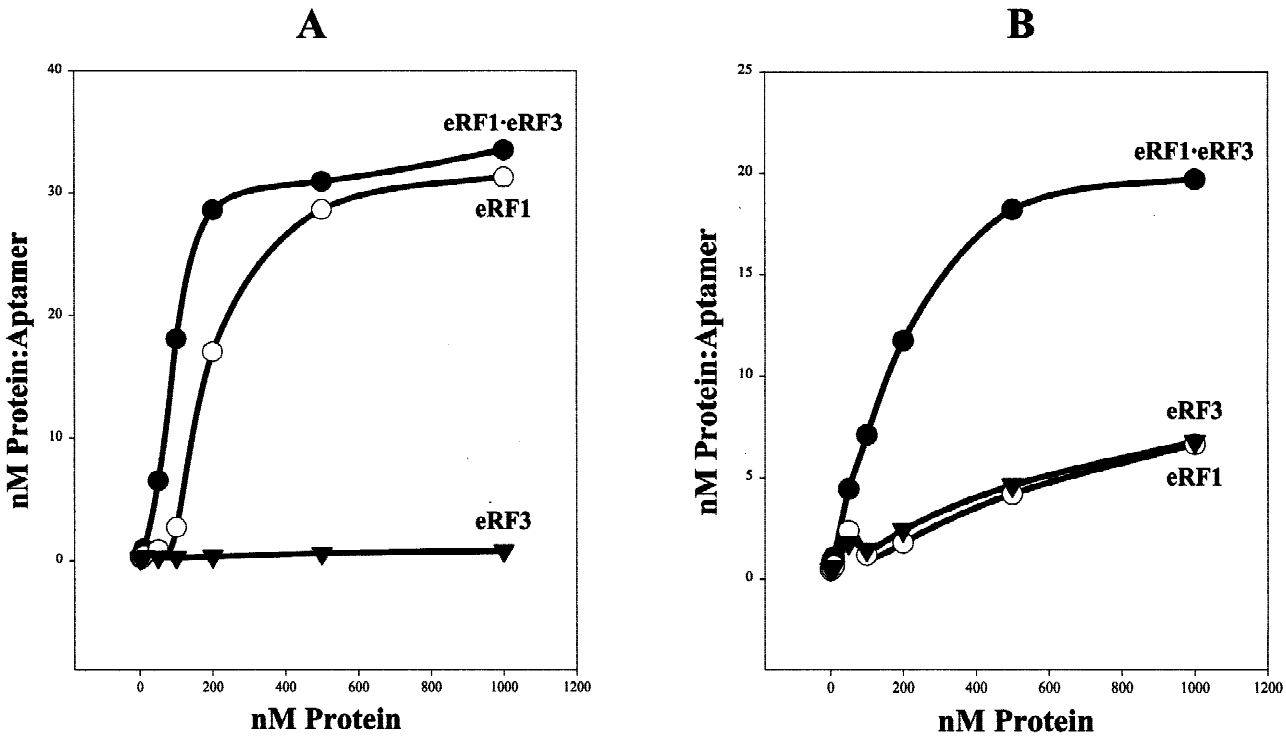

FIGURE 2. **A**: Binding characteristics of Class I eRF1•eRF3 aptamer 12. **B**: Binding characteristics of Class II eRF1•eRF3 aptamer 27. Closed circles represent eRF1•eRF3 complex, open circles eRF1 alone, and closed triangles eRF3 alone. Radiolabeled aptamer RNA bound to protein was quantified by Cerenkov scintillation (see Materials and Methods). In each binding reaction, final concentration of RNA was 50 nM.

gions. Thermodynamically optimal structures generated by mfold (Mathews et al., 1999; Zuker et al., 1999) were modified to include information from Pb hydrolysis and S1 nuclease digestion about looped or non-helical regions. Near-optimal secondary structures that are also consistent with chemical data are shown in Figure 3 for eRF1 aptamers 28 and 34 as well as Class I eRF1•eRF3 aptamers 12 and 17, and Class II aptamer RNA 27.

The apparent secondary structures appear entirely consistent with the classification of RNAs by binding characteristics. The irregular hairpin structures of eRF1•eRF3 aptamers 12 and 17 are quite similar in the region of the terminal internal-loop-and-hairpin, as might be expected from their shared primary structure motifs and their primary affinities for eRF1. The secondary structures of these Class I RNAs in turn are quite similar to the family of eRF1-directed aptamers with related sequences and protein-binding capabilities (e.g., RNA 28; Figs. 1 and 3).

The Class II example, RNA 27, appears significantly different in secondary structure. RNA 27 contains the sequences in common with the rest of its family (and therefore its likely binding site) in a complex multihelix junction rather than at the terminus of a hairpin. Although the fold suggested for RNA 27 in Figure 3 is complex, the four predicted loops are each confirmed by susceptibility to the chemical probes, and the three helices by chemical resistance. Thus the drawing is probably a reasonable model for the underlying secondary structure. This distinctive multihelix junction is consistent with the distinct affinity for both subunits and distinct biochemical activities observed for Class II sequences (below).

Activities of human eRF1 and eRF3 in the presence of aptamers

To determine whether bound aptamers inhibited release factor function, they were tested in several standard biochemical assays. Aptamers selected against eRF1 or the eRF1•eRF3 complex were added to an in vitro assay for hydrolysis of a model nascent peptide in the presence of eRF1 (Tate & Caskey, 1990). This assay measures release of radiolabeled fMet from tRNA (which mimics release of a nascent peptide) in the context of the ribosome and stop codon-containing tetramer. Randomized RNAs from the initial selection pool served as controls, and randomized RNA was separately shown not to alter eRF1 activity.

Several aptamers inhibited termination mediated by eRF1 (Tables 1 and 2). The strongest inhibitors of fMet release from the eRF1 selection were aptamers 2, 28, and 34. eRF1 aptamer 19 showed definite inhibition of fMet release, but was less efficient. The most potent eRF1 aptamers are also comparable to eRF1•eRF3

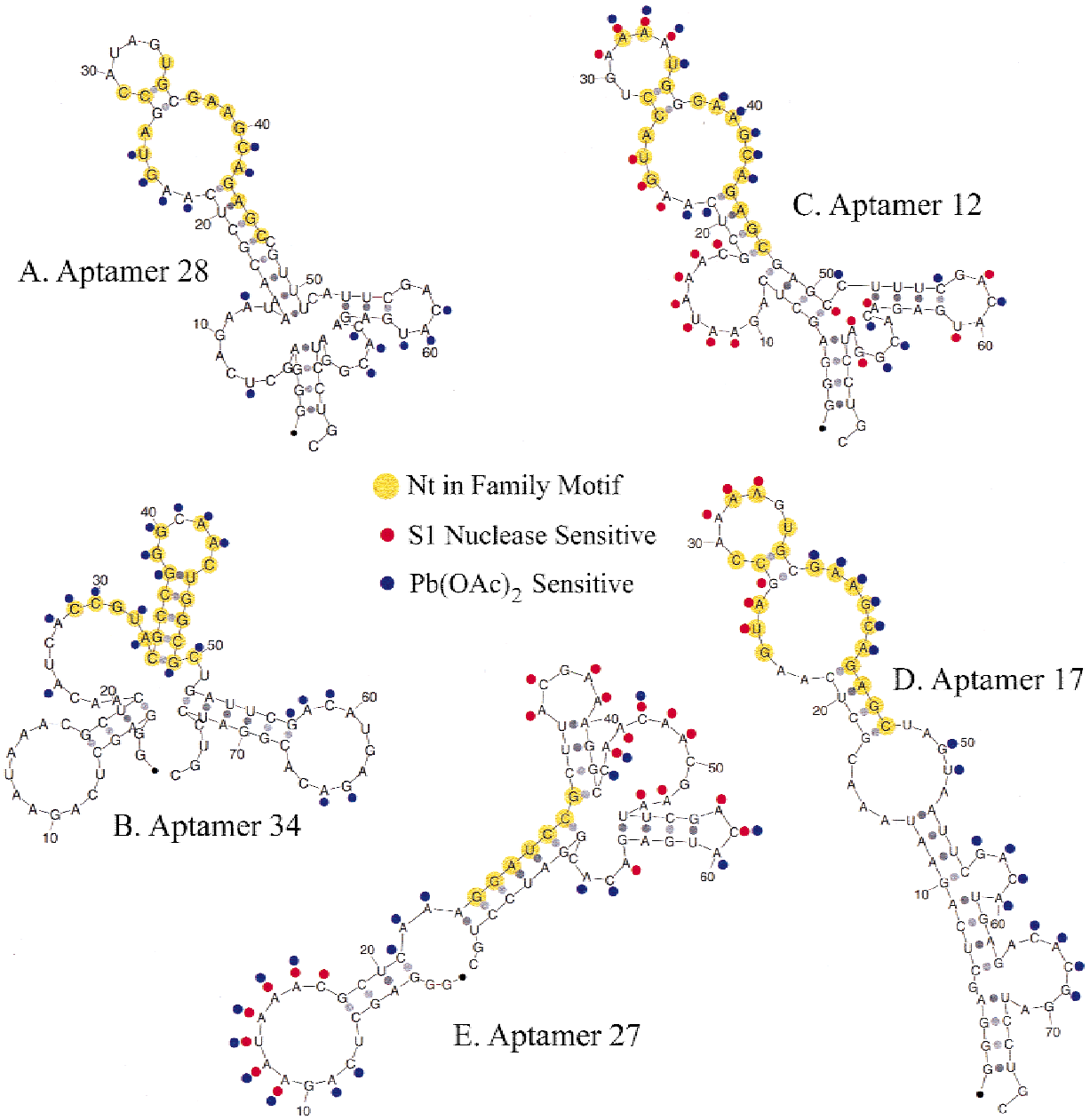

FIGURE 3. **A**: Secondary structure of eRF1 aptamer 28 with predicted $\Delta G = -7.4$ kcal/mol. **B**: Secondary structure of eRF1 aptamer 34 with predicted $\Delta G = -15.6$ kcal/mol. **C**: Secondary structure of eRF1•eRF3 aptamer 12 with predicted $\Delta G = -11.8$ kcal/mol. **D**: Secondary structure of eRF1•eRF3 aptamer 17 with predicted $\Delta G = -9.5$ kcal/mol. **E**: Secondary structure of eRF1•eRF3 aptamer 27 with predicted $\Delta G = -13.9$ kcal/mol. Thermodynamically optimal secondary structures as determined by mfold were modified to include structural information obtained from lead hydrolysis and S1 nuclease digestion. Yellow background indicates nucleotides conserved in independent isolates; red and blue dots indicate nucleotides whose 3′ linkages are sensitive to hydrolysis by S1 nuclease and lead, respectively.

aptamers using this release assay (Table 2). The eRF1•eRF3 aptamers (12 and 17) strongly inhibit fMet release, with activities similar to the best eRF1-selected RNAs. Other eRF1•eRF3 aptamers have no significant effect on release (Table 2). Interestingly, the classification of eRF1•eRF3 aptamers by binding assay is potentially correlated with these release factor activity assays; Class I aptamers inhibited release, but Class II aptamers did not, for any of five sequences tested.

However, Class I binding is not sufficient for inhibition. Class I Aptamer 11 does not obstruct fMet release. However RNA 11 has a distinctly different sequence from 12 and 17 (Fig. 1), and its predicted structure is also quite dissimilar from 12 and 17 (not shown). Such binding without significant effect on release factor activity could indicate the RNA is displaced during termination, or that it occupies a surface that is not employed for normal function.

TABLE 1. RF activity (fMet release) in vitro of human eRF1 in the presence of UAGA and RNA aptamers for human eRF1.[a]

	RF activity, %	
	Molar ratio eRF1:RNA	
RNA aptamer	1:5	1:10
random	100	100
2	13	4
19	44	17
28	4	0
34	8	3

[a]0.08 μM eRF1, 0.4 μ M RNA (1:5 molar ratio) and 0.8 μM RNA-aptamer (1:10). Values shown are an average of at least three independent measurements. Error in individual values estimated to be $\pm$12%.

Effect of aptamers on release factor interactions

At low stop-codon concentrations, eRF1 shows release activity in vitro only when stimulated by eRF3 and GTP (Zhouravleva et al., 1995; Frolova et al., 1996). Such stimulation of eRF1 by eRF3 was only very weakly inhibited (Table 3) by those eRF1-selected aptamers that were strong inhibitors of eRF1 release activity (Table 1). Therefore these aptamers, selected for affinity to eRF1 alone, appear to have little effect on the eRF1•eRF3 interaction. In contrast, the same two Class I eRF1•eRF3 aptamers (12 and 17) that inhibit fMet release also moderately but definitely affect the eRF3-stimulating activity toward eRF1 at low stop-codon concentration (Table 4; note the low concentrations of aptamer used). Other eRF1•eRF3 aptamers appeared to be inactive or marginal inhibitors of eRF3-mediated stimulation of eRF1. Therefore, in contrast to eRF1-directed ligands, some RNAs selected for affinity for the complex eRF1•eRF3 detectably affect the interaction of eRF3 with eRF1.

TABLE 2. RF activity (fMet release) in vitro by human eRF1 in the presence of UAGA stop codon and RNA aptamers to the human eRF1•eRF3 complex.[a]

RNA aptamer	RF activity, %
random	100
1	100
11	106
12	2
17	15
27	95
37	109
C	92
G	97

[a]eRF1 was 0.08 μM, RNA aptamers 0.8 μM (1:10 molar ratio eRF1/RNA). Values shown are an average of at least three independent measurements. Error in individual values estimated to be $\pm$12%.

TABLE 3. Stimulation *in vitro* of human eRF1 by human eRF3 at low stop codon (5 μM UAGA) concentration.[a]

	RF activity, %
RNA aptamer	Molar ratio eRF1:RNA, 1:5
random	100
2	95
19	89
28	80
34	84

[a]Preincubation of the human eRF1 and human eRF1 RNA aptamer at 4 °C for 20 min. Human eRF1 and eRF3 proteins are 0.08 μM, RNA aptamer, 0.4 μM. Values shown are an average of at least three independent measurements. Error in individual values estimated to be $\pm$12%.

The eRF1•eRF3 interaction can also be analyzed by measuring an eRF3 activity (instead of an eRF1 activity) by using intrinsic eRF3-mediated GTP hydrolysis, which requires interaction with eRF1 (Frolova et al., 1996). GTP hydrolysis was not affected by eRF1-directed aptamers, with a possible weak exception for aptamer 28 (Table 5). In contrast, eRF1•eRF3-binding Class I RNAs 12 and 17 definitely inhibit GTPase activity of eRF3 in the presence of ribosomes and eRF1 (Table 6). Other eRF1•eRF3 aptamers were inactive or very weakly active. Thus, inhibition mediated by eRF1-directed aptamers appears relatively specific to hydrolysis of the nascent peptide. A subset of eRF1•eRF3 aptamers, on the other hand, can inhibit both eRF1-mediated fMet–tRNA hydrolysis and eRF3 interactions with eRF1.

Effect of RNA aptamers on translation termination

The ability of eRF1 and eRF1•eRF3 aptamers to inhibit individual release factor activities suggested that they

TABLE 4. Stimulatory activity in vitro of human eRF3 toward human eRF1 at low stop-codon concentration (5 μM UAGA).[a]

	RF activity, %
RNA aptamer	Molar ratio eRF:RNA, 1:1
random	100
1	84
11	87
12	78
17	51
27	109
37	103
C	95
G	113

[a]Human eRF1 and eRF3, 0.08 μM; RNA aptamers to the human eRF1•eRF3 complex, 0.08 μM (molar ratio eRF:RNA, 1:1). Note the lower molar ratio of RNA in these assays; this was required by high background in the absence of GTP with elevated RNA concentrations. Values shown are an average of at least three independent measurements. Error in individual values estimated to be $\pm$12%.

TABLE 5. GTPase activity, using thin-layer chromatography.[a]

RNA aptamer	GTP hydrolysis, %
—	93
random	94
19	98
28	76
34	93

[a]The extent of hydrolysis (%) was calculated as the ratio of radioactivity in the spot corresponding to GDP to the sum of the radioactivity in spots of GTP plus GDP. Human eRF1 and eRF3, 0.4 μM; human eRF1 RNA aptamers, 1.6 μM (1:4 molar ratio eRF1:RNA). Values shown are an average of at least three independent measurements. Error in individual values estimated to be $\pm$12%.

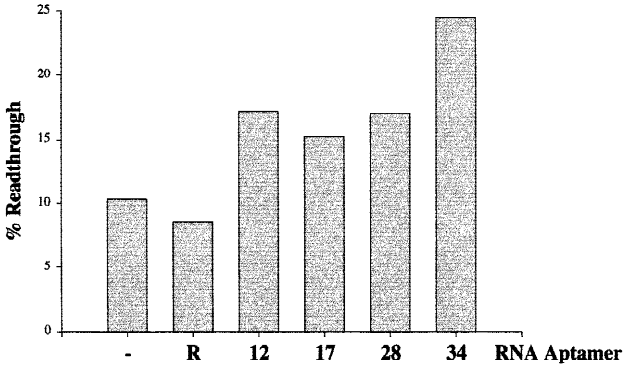

FIGURE 4. RNA aptamers increase readthrough of termination codon UAG. The in vitro translation reaction was performed in the absence or presence of 20 pmol of each RNA aptamer. The results are expressed as percent readthrough of the coat protein UAG terminator. The randomized pool of RNA is denoted as R. The error in individual values is estimated to be $\pm$15%.

might also promote net readthrough of stop codons. That is, these RNAs should slow normal termination. Therefore they will increase the time available for missense readthrough at nonsense codons. Accordingly the fraction of readthrough transits will increase when aptamer is added, provided only that readthrough continues at its initial rate. To detect increases in the fraction of readthrough transits due to eRF inhibition, in vitro translation of tB218-UAG mRNA from beet necrotic yellow vein furovirus was examined.

Translation using the wild-type viral transcript tB218-UAG in reticulocyte extracts yielded clearly detectable readthrough protein (75K) in addition to the coat protein (22K) itself. A typical experiment demonstrating the effect of RNA aptamers is shown in Figure 4. Control (randomized) RNA sequences had no effect on readthrough in vitro. However, addition of eRF1 aptamers 28 or 34, or eRF1•eRF3 Class I aptamers 12 or 17 to the incubation mixture increased readthrough to the range from 15.2% to 24.5%. Consequently, eRF1 aptamers 28 and 34, as well as eRF1•eRF3 aptamers 12 and 17, behave as antiterminators in this system, presumably acting via their selected inhibition of endogenous rabbit eRF1 present in the reticulocyte lysate.

TABLE 6. GTPase activity using thin-layer chromatography.[a]

	TGTP hydrolysis, %	
	Molar ratio eRF:RNA	
RNA aptamers	1:2	1:4
none	86	
random	97	81
1	97	72
11	96	75
12	55	39
17	63	57
27	98	92
37	98	100
C	78	69
G	83	61

[a]Percent GTP hydrolysis was calculated as the ratio of radioactivity in the spot corresponding to GDP to the sum of the radioactivity in GTP plus GDP. GTP, 5 μM; Human eRF1 and eRF3, 0.4 μM; RNA aptamers to eRF1•eRF3 complex, 0.8 and 1.6 μM. Preincubation of eRF1 plus eRF3 plus aptamer for 20 min at 4 °C. Values shown are an average of at least three independent measurements. Error in individual values estimated to be $\pm$12%.

Effect of RNA aptamers on eRF1-induced termination

To confirm that aptamer-mediated readthrough occurs via inhibition of eRF1, exogenous purified human eRF1 was added to in vitro translation reactions. Added eRF1 reduced readthrough about fourfold in the in vitro translation of tB218-UAG mRNA. Thus exogenous human eRF1 is functional and observably in competition with readthrough translation in this system.

RNA aptamers were then added to in vitro translations in which readthrough had been reduced by the addition of exogenous human eRF1 (Fig. 5). This low level of readthrough (2.5%) was not significantly altered by randomized RNAs, where 3.2% readthrough was measured. In contrast, inclusion of eRF1 aptamers 28 or 34 or eRF1•eRF3 aptamers 12 or 17 virtually re-established the original level of readthrough that now reached 7.2–12.6%. Thus the effect of added human eRF1 protein was almost completely reversed by human eRF aptamers.

Similar experiments were carried out with purified *Xenopus* eRF1 added to reticulocyte lysates, with parallel results (data not shown). These same four RNAs therefore inhibit *Xenopus* release factor eRF1 also. We conclude that some RNAs selected for affinity to release factor inhibit individual biochemical activities of both eRF1 and eRF3, and ultimately suppress translation termination on eukaryotic ribosomes.

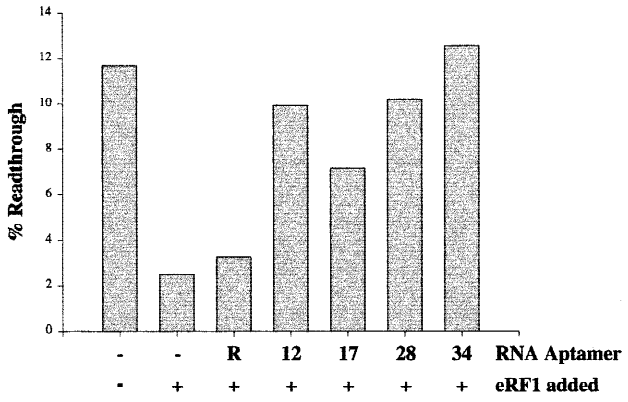

FIGURE 5. RNA aptamers prevent human eRF1-induced termination. The conditions are as in Figure 4, except that, where indicated, incubations were carried out in the presence of 40 pmol of each RNA aptamer, and 4 pmol of human eRF1. The randomized pool of RNA is denoted as R. The results are expressed as percent readthrough, as in Figure 4. The error in individual values is estimated to be ±15%.

DISCUSSION

We have observed inhibition of eRF1 and eRF1•eRF3 activities by RNAs selected for affinity to the RF proteins. Because the eRF1 protein family is highly conserved (Frolova et al., 1994; Kisselev et al., 2000), and because we have observed activity against purified *X. laevis* (see Materials and Methods), rabbit proteins (Fig. 4) and purified human eRF1 (Fig. 5), we expect inhibition of a broad group of eukaryotic eRF1s. Prokaryotic RF1 and RF2 differ in sequence (Kisselev et al., 2000) from eukaryotic factor eRF1 with the exception of small conserved motifs (e.g., GGQ; Frolova et al., 1999). Therefore these present RNA ligands will probably inhibit only eukaryotic termination.

Structures of the reactants

The actions of RNAs in release factor assays can be related to the structures of the proteins and the selected RNAs. RF1, RF2, and eRF1 are RNA-binding proteins, and have in particular, affinity for termination codons. Photoactivated termination codons containing 4-thiouridine (s^4U; reviewed in Favre & Fourrey, 1995; Favre et al., 1998) in the first position can be used to demonstrate this interaction. In *Escherichia coli* ribosomes, s^4UAA-containing 36-mer mRNA was shown to crosslink to the ribosomal RNA and with low efficiency to RF2 (Tate et al., 1990). With s^4UGAN instead of s^4UAAN the yield of crosslinks between RF2 and s^4UGAN increased (Brown & Tate, 1994). The identity of the fourth base in the stop signal also strongly affected the interaction with RF. Further analysis demonstrated that three positions after the stop codon were able to crosslink to *E. coli* RF2, though the efficiency of crosslinking from the +1 nucleotide was much higher than from +4 and +6 (Poole et al., 1997, 1998). In addition, particular adjacent amino acid sequence changes within bacterial RF1 and RF2 alter the codon triplets translated as stop (Ito et al., 2000), suggesting that bacterial RF is in contact with stop codon nucleotides. Within eukaryotic ribosomes, the proximity of stop codons and human eRF1 has been similarly demonstrated using the photocrosslinking strategy (L. Chavatte, L. Frolova, L. Kisselev, and A. Favre, unpubl.).

Ribosomal RNA is also close to RF. A region of 16S ribosomal RNA has been found to crosslink to the RF. For prokaryotic ribosomes genetic evidence also implicates ribosomal RNAs in translation termination (Arkov et al., 1998). Moreover, the prokaryotic ribosomal A site where RF1/2 interacts can now be seen to be predominantly composed of ribosomal RNA (Ban et al., 1999; Cate et al., 1999).

Release factors are therefore highly specialized proteins designed for an environment replete with RNAs. Interference with any natural RNA site by a competing RNA would inhibit termination. However, interference need not be specific. General steric interference with ribosomal entry by a large polyanionic ligand like a tightly-bound RNA would presumably also disrupt termination.

The unique structure of eRF1, like a three-lobed star, is thought to promote the multiple known release factor functions. Taking the leftward lobe as the site of contact with the stop codon, the downward lobe has been suggested as the site of communication to the peptidyl transferase center (Song et al., 2000). Human eRF1 has also been biochemically divided into two unequal functional regions: the "core" NM domain encompasses the N-terminal and M (middle) parts of the eRF1 chain (Frolova et al., 2000). The core NM domain (275 ± 5 amino acids) is enriched in basic amino acids (pI 9.74) and is fully active in triggering fMet-$tRNA^{Met}$ hydrolysis on the ribosome at high stop-codon concentration. N and M are also the leftward and downward lobes of the star (Song et al., 2000). The C-terminal domain is involved in eRF3 binding (Merkulova et al., 1999) and is also the distinct, rightward-pointing lobe of the eRF1 star, whose overall shape has been compared to tRNA (Song et al., 2000).

Inhibition of nascent peptide release

This underlying human eRF1 structure (Song et al., 2000) suggests a location for the aptamer sites. We suggest that the eRF1-directed RNAs (e.g., RNA 28; Figs. 1 and 3) and the sequence-related class I eRF1•eRF3 RNAs (e.g., RNAs 12 and 17) are directed to the NM (leftward and downward) domains that are competent for release activity alone. These areas would provide the constant target for RNA binding suggested by the similar structures of the eRF1 and Class I RNAs,

and occupation of this site would explain inhibition of release (Tables 1 and 2).

The availability of RNAs binding this NM domain target from two different selections may have further implications. For example, the RNA 12–17 Class I family is part of such a set of aptamers. Here the eRF1•eRF3 selection independently yielded a structure paralleling an eRF1 motif (compare RNA 28), but changed in three ways (Figs. 1 and 3). First, constraints visible in the eRF1 loops become invariant in the eRF1•eRF3 loops (e.g., the conserved CC and UG sequences; Fig. 1). In addition, the loops themselves become notably more homogeneous. Finally, the RNA hairpin loops targeted to the eRF1•eRF3 complex now conserve a tract of As within the loop (Figs. 1 and 3) absent from the related eRF1 RNAs. These differences might be explained by a single hypothesis if eRF1•eRF3 aptamers have added to their basic NM domain (left/downward) binding sites just at or beyond the limit reached by the comparable eRF1 aptamers. Thus we suggest the extended activity of the Class I eRF1•eRF3 RNAs is due to the extension of the terminal hairpin (Fig. 3) toward the eRF1•eRF3 interface, where the observed interference with eRF1-eRF3 interaction can occur. This notion also accounts for the somewhat tighter binding of the eRF1•eRF3 aptamers.

Interaction with eRF3

In contrast to eRF1, Class 2 RFs (RF3 and eRF3) do not act as ribonucleoproteins. Instead they are GTP-binding proteins (Grentzmann et al., 1994; Mikuni et al., 1994; Zhouravleva et al., 1995) that hydrolyze the triphosphate when bound to the ribosome (Frolova et al., 1996; Freistroffer et al., 1997; Grentzmann et al., 1998; Pel et al., 1998). Interaction with eRF1 is essential for eRF3 GTPase, via contacts between their C-termini (Ebihara & Nakamura, 1999; Merkulova et al., 1999). Such eRF1•eRF3 complexes are evident both in vivo and in vitro (Stansfield et al., 1995; Zhouravleva et al., 1995; Paushkin et al., 1997). Thus, although eRF3 is probably not a natural RNA-binding protein, we still expect surfaces with potential RNA affinity on the protein. RNAs with high affinities can be selected to virtually every protein, even toward peptide domains that lack natural sites for ribonucleotides or other polyanions (Gold et al., 1995).

Our selection yielded RNAs that definitely contact eRF3. These are the Class II RNAs like RNA 27 (Figs. 1 and 3) that have a unique multihelix-junction structure and complementary affinities for eRF1 and eRF3 alone (Fig. 2). We suggest that these RNAs actually bridge the eRF1•eRF3 interface in the rightward (C domain; carboxyl-terminal) domain of the eRF1 structure (Song et al., 2000). Such a distinct site would be consistent with the observed unique primary and secondary structures, which differ from Class I and eRF1 aptamers (Figs. 1 and 3). However, Class II RNAs do not inhibit RF activity (Table 2). Because Class II RNAs were selected against the heterodimer, their binding may be consistent with a functional eRF1•eRF3 interface. Thus, they may allow functional interactions between the RF proteins, as well as continued release function by the relatively distant NM domain.

Nature of inhibition

RNA-binding proteins sometimes predominantly bind selected RNAs to their normal RNA sites. A eukaryotic translation initiation factor—eIF4B—contains an RNA-recognizing motif (RRM) that interacts with ribosomal 18S RNA. When used to select RNA aptamers in vitro (Methot et al., 1996), it appeared that selected aptamers inhibit the binding of RRM to the ribosomal RNA. Similarly, RNAs selected to bind to the Sex-lethal splicing regulator protein are found to contain a polypyrimidine tract like that found in mRNAs whose splicing is regulated (Singh et al., 1995). However, this is not always observed: RNAs with selected affinity for SelB, which binds both mRNA and tRNA, do not notably resemble normal ligands (Klug et al., 1999). Nevertheless, we have followed this thought, looking for sequence similarities to the natural RNAs that bind RFs in our selected oligomers. Although termination codons, CCA sequences, and small ribosomal RNA homologies do occur in these aptamers, they are not statistically prominent. Furthermore, protein surfaces that are not normally RNA sites can yield among the highest affinities for selected aptamers (Gold et al., 1995). Thus, more specific structural data for the RNA–protein complexes will be needed to define a detailed mechanism of release factor inhibition by these selected RNAs.

Application and extension of these findings

How can RF-specific aptamers be used in experimental biology? Some applications are easily foreseen. First, they are new experimental reagents for the study of termination in vitro. For example, by adding such aptamers to an in vitro translation system, one may stall translating ribosomes without, or with slowed, release of the nascent polypeptide chain from the ribosome. This will likely enhance aberrant translation outcomes, like readthrough and/or frameshifting at the termination codon. The inhibited reactions may be a practical means of preparing the natural substrate for the termination reaction itself. In addition, these RNAs are likely to be omnipotent suppressors of eukaryotic termination. Because eRF1 and eRF3 are involved in the "surveillance complex" that triggers nonsense-codon-mediated mRNA decay (Czaplinski et al., 1998) RF aptamer RNAs may modulate the stability of mRNAs with nonsense mutations. Finally, it may be possible to implement a universal therapy for genetic disease re-

sulting from premature translation termination by expressing release factor aptamers at high levels in vivo, and thereby suppressing human nonsense mutations within essential genes.

MATERIALS AND METHODS

Selection-amplification

Two independent selections were performed, one using human eRF1 alone as the target for RNA, and another using the complex of human eRF1•eRF3 as the target.

Protein preparations

For eRF1 selection, human eRF1 terminated at Tyr-415 ($eRF1^{1-415}$) was used as the affinity reagent. Cloning and expression of cDNA encoding the human $eRF1^{1-415}$ has been described (Merkulova et al., 1999). Human $eRF1^{1-415}$ is fully active in all RF assays, including those for release and GTPase. Purification of human $eRF1^{1-415}$ containing a His-tag was performed on a Ni-NTA-agarose (Qiagen) column, as follows. *E. coli* (TG1 strain, Qiagen) expressing human $eRF1^{1-415}$ were pelleted at 4 °C and resuspended in sonication buffer (50 mM Na_2HPO_4, 300 mM NaCl, 10 mM 2-mercaptoethanol, Complete™ protease inhibitor (Boehringer-Mannheim), pH 7.8) and lysed by sonication on ice. Lysed *E. coli* were centrifuged at 16,000 × *g* (4 °C for 20 min) and the supernatant loaded on a Ni-NTA-agarose column. Bound eRF1 was washed with sonication buffer + 20 mM imidazole, and eluted in sonication buffer + 250 mM imidazole, substituting 1 mM phenyl methyl sulfonyl fluoride for Complete™ protease inhibitor. Imidazole was removed from purified eRF1 using a NAP-5 column (Pharmacia Biotech) before selection.

For heterodimer selections and for in vitro RF assay and GTPase activity assay, human eRF1 and eRF3 purified from the baculovirus system were used. Subcloning of the human eRF1 and eRF3, expression of both factors in the baculovirus expression system, and purification of the human eRF1 and eRF3 using ion-exchange chromatography have been described (Frolova et al., 1998).

The human eRF1•eRF3 protein complex was generated in vitro. Equimolar amounts of eRF3 and eRF1 were incubated in 0.15 M KCl, 50 mM Tris-HCl, pH 7.2, and 1 mM $MgCl_2$ for 0.5 h at 4 °C.

RNA preparations

Initial RNA pools of $>10^{14}$ unique randomized sequences were generated by T7 transcription of the following primed 102-mer template: 5′-ccgaa gct**ta atacg actca ctata ggg**ag ctcag aataa acgct caa -N_{30} -ttcga catga gacac ggatc ctgc-3′, where N_{30} represents 30 randomized nucleotide positions (T7 promoter in bold text). All RNA transcriptions incorporated [α-^{32}P]-CTP to allow quantitative monitoring of the selection.

Selection for aptamers binding to eRF1

RNA sequences bound to human eRF1 were isolated by filter binding using mixed cellulose ester MF-Millipore filters (catalog #HAWP02500). RNA pools were prepared for selection by passage through two filters in the absence of protein to eliminate filter-binding RNAs. Then each round of selection comprised three binding reactions containing 0, 15, or 60 pmol eRF1 and 750 pmol RNA incubated at 37 °C for 4 min in 200 μL binding buffer (20 mM Tris, pH 7.5, 2 mM $MgCl_2$, 40 mM NH_4Cl, 10 mM KCl). MF-Millipore filters in a Millipore 1225 sampling manifold were prewashed with 1 mL of binding buffer, the binding reaction was applied, and the filters were washed with 2 mL binding buffer. RNA retained on the filter was detected by Cerenkov scintillation. The filter with the greatest ratio of bound radioactivity to a control with no protein was carried forward. RNA was extracted from this filter with 1 mL of a 2:1 mixture of phenol (equilibrated to pH 8):8 M urea at room temperature for 30 min. Water (400 μL) was added and the aqueous phase was ethanol precipitated and RNA was resuspended in water. Reverse transcription and PCR amplification were performed by standard methods (e.g., Ciesiolka et al., 1996). After nine rounds of selection, cDNAs of the selected pool of RNAs were digested with *Bam*HI and *Hin*dIII, cloned into the matching sites of pGEM3Zf+ (Promega), and sequenced (Fig. 1A).

Selection for aptamers binding to eRF1•eRF3 complex

Rounds 1 through 3 of selection for eRF1•eRF3 binding utilized filter binding, as described above. Each round included three binding reactions, with 0, 15, or 60 pmol eRF1•eFR3 complex and 750 pmol RNA, incubated for 4 min at 37 °C in 1 mM $CaCl_2$, 10 mM $MgCl_2$, 140 mM KCl, 1 mM GTP, 10 mM NaCl, and 20 mM HEPES, pH 7.2. A rising background of filter binding (without protein) was evident in the third round. Rounds 4 and 5 were therefore performed using an electrophoretic gel mobility shift selection. After the same binding reactions, sucrose was added to a final concentration of 10% and the reaction loaded onto a nondenaturing 8% polyacrylamide gel formed in the binding buffer. The gel was run at 37 °C and RNAs that migrated more slowly than a control band (run in the absence of protein) were excised and eluted. Two such electrophoretic selections eliminated the filter background. Rounds 6 through 9 were carried out using the filter-binding method. The cDNAs of the selected round 9 RNAs were cloned using blunted DNA termini into pT7Blue-3 (Novagen) and sequenced (Fig. 1B).

Measurement of binding

Apparent dissociation constants were calculated by least square fits of filter selection data using SigmaPlot (Jandel Scientific Software, San Rafael, California). As previously described for filter selection, binding of radiolabeled RNA to a molar excess of the protein target was allowed to equilibrate for 4 min at 37 °C, then the binding reaction was passed over a MF-Millipore filter. RNA was quantified by Cerenkov scintillation.

RNA structure analysis

RNA secondary structure was probed by lead hydrolysis and S1 nuclease digestion (e.g., as described in Illangasekare &

Yarus, 1999) with the following modifications. For eRF1 aptamers, lead hydrolysis was performed at 22 °C for 15 min. Final concentrations of $Pb(OAc)_2$ were 0.05, 0.1, 0.25, and 0.5 mM. For eRF1•eRF3 aptamers, lead hydrolysis took place at 37 °C for 4 min, with final concentrations of $Pb(OAc)_2$ being 0, 2, 4, 8, 12, and 20 μM. S1 nuclease digestion took place at 37 ° C for 1–4 min, using 0, 1, 5, 15, and 30 U of S1 nuclease.

In vitro RF assay

Purified eRF1 and eRF3 activities were measured as described (Caskey et al., 1974; Frolova et al., 1994; Zhouravleva et al., 1995). The release activity of eRF1 alone was measured at saturation levels (50 μM) of the stop-codon-containing tetranucleotide UAGA, and GTP was not included in the reaction mixture. RF-stimulating activity of eRF3 towards eRF1 was measured at a nonsaturation level (5 μM) of UAGA in the presence of 0.1 mM GTP. The incubation mixture (25 μL) contained 20 mM Tris-HCl, pH 7.5, 15 mM $MgCl_2$, 8 mM NH_4Cl, 1.5 pmol f[^{35}S]Met-tRNA^{fMet}-AUG-ribosome complex. Where indicated, eRF1 alone or the mixture of eRF1 and eRF3 was added.

To measure the influence of RNA aptamer on RF activity of eRF1 or RF-stimulating activity of eRF3 toward eRF1, both factors were preincubated with RNA for 20 min at 4 °C and then added to the incubation mixture. RNA from the initial random pool was used as a negative control. The value of f[^{35}S]Met released in the absence of the stop codon (for eRF1 alone) or of GTP (for the stimulating activity of eRF3 toward eRF1) was subtracted from assay values. Rabbit ribosomal subunits were purified as described (Frolova et al., 1998).

Assay for GTPase activity

GTPase activity was followed by accumulation of [^{32}P]GDP after hydrolysis of [α-^{32}P]-GTP using thin-layer chromatography on PEI-cellulose-coated plates (Macherey-Nagel; Frolova et al., 1996). Incubation mixtures (12.5 μL) contained 5 μM [α-^{32}P]-GTP (Amersham; specific activity: 5,000 cpm/pmol) and 0.1 μM of rabbit ribosomes, eRF1, eRF3, and RNA aptamer as indicated. RNA from the initial random pool was used as a negative control. The reaction was stopped by addition of 1 μL of 20 mM EDTA and 5% SDS. Five-microliter aliquots were spotted onto PEI-cellulose plates and resolved in 1 M acetic acid and 1 M LiCl for 1.5 h. The plates were dried and exposed to X-ray film (Hyperfilm^{TM}-MP, Amersham). Percent GTP hydrolysis was calculated as the ratio of radioactivity in the spot corresponding to GDP to the sum of the spots of GTP plus GDP $\times$ 100.

Production of mRNA and translation in vitro

Plasmid pB218-TAG was used for as the source of mRNA. It includes a fragment corresponding to wild-type beet necrotic yellow vein furovirus RNA 2 (nt 1–2715), which comprises the 5′ untranslated region, the coat protein and readthrough domain, and 495 nt following the UAG termination codon separating the coat protein from the readthrough domain. The corresponding capped transcript (tB218-UAG) was synthesized and used as mRNA for in vitro translation in a rabbit reticulocyte lysate. Translation products were internally labeled with ^{35}S methionine and cysteine. The activity of 20 pmol of aptamers was tested in the absence or presence of 2 pmol of *Xenopus laevis* eRF1 (data not shown) per incubation reaction, or 40 pmol of aptamers were tested with 4 pmol of human eRF1. RNA from the initial random pool was used as a negative control. The translation products were analyzed by gel scanning (Drugeon et al., 1997) using the National Institutes of Health (NIH) image program, or the relevant bands A (readthrough protein: 75K) and B (coat protein: 22K) were excised from a dried gel and counted. Raw data were normalized for the number of potential sites for ^{35}S incorporation in 75K and 22K proteins. The results are expressed as 100 times values obtained for A over the values obtained for A + B. Scanning and excising bands yielded comparable results.

ACKNOWLEDGMENTS

We are thankful to X. LeGoff (Rennes) for aid in purification of eRF1 and I. Bjørndal (Aarhus) for cultivation of insect cells. This work was supported by the Human Frontier Science Program (Grant R96-032), by Programme Internationale Cooperation Scientifique du Centre National de la Recherche Scientifique (CNRS), by the Russian Foundation for Basic Research, by Chaire Internationale Blaise Pascale via Ecole Normale Supérieure, and by NIH Research Grants GM 30881 and GM 48080 to M.Y. and HL65610 to L.L. and finally, the Colorado RNA Center. The Institut Jacques Monod is an Institut Mixte, CNRS, Universités Paris 6 & 7.

Received July 7, 2000; returned for revision July 18, 2000; revised manuscript received July 26, 2000

REFERENCES

Arkov AL, Freistroffer DV, Ehrenberg M, Murgola EJ. 1998. Mutations in RNAs of both ribosomal subunits cause defects in translation termination. *EMBO J 17*:1507–1514.

Ban N, Nissen P, Hansen J, Capel M, Moore PB, Steitz TA. 1999. Placement of protein and RNA structures into a 5 Å-resolution map of the 50S ribosomal subunit. *Nature 400*:841–847.

Brown CM, Tate WP. 1994. Direct recognition of mRNA stop signals by *Escherichia coli* polypeptide chain release factor two. *J Biol Chem 269*:33164–33170.

Buckingham RH, Grentzmann G, Kisselev L. 1997. Polypeptide chain release factors. *Mol Microbiol 24*:449–456.

Cantor C. 1979. tRNA-ribosome interactions. In: Scimmel P, Soll D, Abelson J, eds. *Transfer RNA: Structure, properties and recognition*. Cold Spring Harbor, New York: Cold Spring Harbor Laboratory Press. pp 363–392.

Caskey CT, Beaudet AL, Tate WP. 1974. Mammalian release factor: In vitro assay and purification. *Methods Enzymol 30*:293–303.

Cate JH, Yusupov MM, Yusupova GZ, Earnest TN, Noller H. 1999. X-ray crystal structures of 70S ribosome functional complexes. *Science 285*:2095–2104.

Ciesiolka J, Illangasekare M, Majerfeld I, Nickles T, Welch M, Yarus M, Zinnen S. 1996. Affinity selection from randomized ribonucleotide pools. *Methods Enzymol 267*:315–335.

Curran JF, Yarus M. 1988. Use of tRNA suppressors to probe regulation of *E. coli* release factor 2. *J Mol Biol 203*:75–83.

Czaplinski K, Ruiz-Echevarria MJ, Paushkin SV, Han X, Weng Y, Perlick HA, Dietz HC, Ter-Avanesyan MD, Peltz SW. 1998. The surveillance complex interacts with the translational release factors to enhance termination and degrade aberrant mRNAs. *Genes & Dev 12*:1665–1677.

Drugeon G, Jean-Jean O, Le Goff X, Frolova L, Philippe M, Kisselev L, Haenni A-L. 1997. Eukaryotic release factor 1 (eRF1) abolishes read-through and competes with suppressor tRNAs at all three codons in termination messenger RNA. *Nucleic Acids Res 25*:2254–2258.

Ebihara K, Nakamura Y. 1999. C-terminal interaction of translational release factors eRF1 and eRF3 of fission yeast: G-domain un-

coupled binding and the role of conserved amino acids. *RNA 5*:739–750.
Eggertsson G, Soll P. 1988. Transfer RNA-mediated suppression of termination codons in *E. coli. Microbiol Rev 52*:354–379.
Favre A, Fourrey J-L. 1995. Structural probing of small endonucleolytic ribozymes in solution using thio-substituted nucleobases as intrinsic photolabels. *Acc Chem Res 28*:375–382.
Favre A, Saintome C, Fourrey J-L, Clivio P, Laugaa P. 1998. Thionucleobases as intrinsic photoaffinity probes of nucleic acid structure and nucleic acid-protein interactions. *J Photochem Photobiol 42*:109–124.
Freistroffer DV, Pavlov MYu, MacDougall J, Buckingham RH, Ehrenberg M. 1997. Release factor RF3 in *E. coli* accelerates the dissociation of release factors RF1 and RF2 from the ribosome in a GTP-dependent manner. *EMBO J 16*:4126–4133.
Frolova L, Le Goff X, Rasmussen HH, Cheperegin S, Drugeon G, Kress M, Arman I, Haenni A-L, Celis JE, Philippe M, Justesen J, Kisselev L. 1994. A highly conserved eukaryotic protein family possessing properties of polypeptide chain release factor. *Nature 372*:701–703.
Frolova L, Le Goff X, Zhouravleva G, Davydova E, Philippe M, Kisselev L. 1996. Eukaryotic polypeptide chain release factor eRF3 is an eRF1- and ribosome-dependent guanosine triphosphatase. *RNA 2*:334–341.
Frolova LYu, Simonsen JL, Merkulova TI, Litvinov DY, Martensen PM, Rechinsky VO, Camonis J, Kisselev LL, Justesen J. 1998. Functional expression of eukaryotic polypeptide chain release factors 1 and 3 by means of baculovirus/insect cells and complex formation between the factors. *Eur J Biochem 256*:36–44.
Frolova LYu, Tsivkovskii R, Sivolobova G, Oparina N, Serpinsky O, Blinov V, Tatkov S, Kisselev L. 1999. Mutations in the highly conserved GGQ motif of class 1 polypeptide release factors abolish ability of human eRF1 to trigger peptidyl-tRNA hydrolysis. *RNA 5*:1014–1020.
Frolova LYu, Merkulova T, Kisselev L. 2000. Eukaryotic polypeptide release factor eRF1 is composed of two functionally and structurally distinct domains. *RNA 6*:381–390.
Gold L, Polisky B, Uhlenbeck O, Yarus M. 1995. Diversity of oligonucleotide function. *Annu Rev Biochem 64*:763–797.
Grentzmann G, Brechemier-Baey D, Heurgue V, Mora L, Buckingham RH. 1994. Localization and characterization of the gene encoding release factor RF3 in *Escherichia coli. Proc Natl Acad Sci USA 91*:5848–5852.
Grentzmann G, Kelly PJ, Laalami S, Shuda M, Firpo MA, Cenatiempo Y, Kaji A. 1998. Release factor RF-3 GTPase activity acts in disassembly of the ribosome termination complex. *RNA 4*:973–983.
Hüttenhofer A, Böck A. 1998. Selenocysteine inserting RNA elements modulate GTP hydrolysis of elongation factor SelB. *Biochemistry 37*:885–890.
Illangasekare M, Yarus M. 1999. Specific, rapid synthesis of pheRNA by RNA. *Proc Natl Acad Sci USA 96*:5470–5475.
Ito K, Ebihara K, Uno M, Nakamura Y. 1996. Conserved motifs of prokaryotic and eukaryotic polypeptide chain release factors: tRNA–protein mimicry hypothesis. *Proc Natl Acad Sci USA 93*:5443–5448.
Ito K, Uno M, Nakamura Y. 2000. A tripeptide "anticodon" deciphers stop codons in messenger RNA. *Nature 403*:680–684.
Kisselev LL, Oparina NY, Frolova LY. 2000. Class-1 polypeptide release factors are structurally and functionally similar to tRNAs and comprise different structural-functional families of prokaryotic/mitochondrial and eukaryotic/archaebacterial factors. *Mol Biol* (Moscow) *34*:427–442.
Klug S, Hüttenhofer A, Famulok M. 1999. In vitro selection of RNA aptamers that bind special elongation factor SelB, a protein with multiple RNA-binding sites, reveals one major interaction domain at the carboxyl terminus. *RNA 5*:1180–1190.
Le Goff X, Philippe M, Jean-Jean O. 1997. Overexpression of human release factor 1 alone has a antisuppressor effect in human cells. *Mol Cell Biol 17*:3164–3172.
Mathews DH, Sabina J, Zuker M, Turner DH. 1999. Expanded sequence dependence of thermodynamic parameters improves prediction of RNA secondary structure. *J Mol Biol 288*:911–940.
Merkulova TI, Frolova LY, Lazar M, Camonis J, Kisselev L. 1999. C-terminal domains of human translation termination factors eRF1 and eRF3 mediate their in vivo interaction. *FEBS Lett 443*:41–47.
Methot N, Pickett G, Keene JD, Sonenberg N. 1996. In vitro RNA selection identifies RNA ligands that specifically bind to eukaryotic translation initiation factor 4B: The role of the RNA recognition motif. *RNA 2*:38–50.
Mikuni O, Ito K, Moffat J, Matsumura K, McCaughan K, Nobukuni T, Tate W, Nakamura Y. 1994. Identification of the *prfC* gene, which encodes peptide-chain release factor 3 of *Escherichia coli. Proc Natl Acad Sci USA 91*:5798–5802.
Moffat JG, Tate WP. 1994. A single proteolytic cleavage in release factor 2 stabilizes ribosome binding and abolishes peptidyl-tRNA hydrolysis activity. *J Biol Chem 269*:18899–18903.
Nakamura Y, Ito K, Isaksson LA. 1996. Emerging understanding of translation termination. *Cell 87*:147–150.
Nakamura Y, Ito K. 1998. How proteins read the stop codon and terminates translation. *Genes to Cells 3*:265–278.
Nissen P, Kjeldgaard M, Thirup S, Polekhina G, Reshetnikova L, Clark BE, Nyborg J. 1995. Crystal structure of the ternary complex of Phe-tRNAPhe, EF-Tu, and a GTP analog. *Science 270*:1464–1472.
Nyborg J, Nissen P, Kjeldgaard M, Thirup S, Polekhina G, Clark B. 1996. Structure of the ternary complex of EF-Tu: Macromolecular mimicry in translation. *Trends Biochem Sci 21*:81–82.
Paushkin SV, Kushnirov VV, Smirnov VN, Ter-Avanesyan MD. 1997. Interaction between yeast Sup45p (eRF1) and Sup35p (eRF3) polypeptide chain release factors: Implications for prion-dependent regulation. *Mol Cell Biol 17*:2798–2805.
Pel HJ, Moffat JG, Ito K, Nakamura Y, Tate WP. 1998. *Escherichia coli* release factor 3: Resolving the paradox of a typical G protein structure and atypical function with guanine nucleotides. *RNA 4*:47–54.
Poole ES, Brimacombe R, Tate WP. 1997. Decoding the translational termination signal: The polypeptide chain release factor in *Escherichia coli* crosslinks to the base following the stop codon. *RNA 3*:974–982.
Poole ES, Major LL, Mannering SA, Tate WP. 1998. Translational termination in *Escherichia coli*: Three bases following the stop codon crosslink to release factor 2 and affect the decoding efficiency of UGA-containing signals. *Nucleic Acids Res 26*:954–960.
Selmer M, Al-Karadaghi S, Hirokawa G, Kaji A, Lilias A. 1999. Crystal structure of *Thermotoga maritima* ribosome recycling factor: A tRNA mimic. *Science 286*:2349–2352.
Singh R, Valarcel J, Green MR. 1995. Distinct binding specificities and functions of higher eukaryotic polypyrimidine tract-binding proteins. *Science 268*:1173–1176.
Song H, Mugnier P, Das AK, Webb HM, Evans DR, Tuite MF, Hemmings BA, Barford D. 2000. The crystal structure of human eukaryotic release factor eRF1: Mechanism of stop codon recognition and peptidyl-tRNA hydrolysis. *Cell 100*:311–321.
Stansfield I, Jones KM, Kushnirov VV, Dagkesamanskaya AR, Poznyakovski AI, Paushkin SV, Nierras CR, Cox BS, Ter-Avanesyan MD, Tuite MF. 1995. The products of the *SUP45* (eRF1) and *SUP35* genes interact to mediate translational termination in *Saccharomyces cerevisiae*. *EMBO J 14*:4365–4373.
Tate WP, Caskey CT. 1990. Termination of protein synthesis. In: Speding G, ed. *Ribosomes and protein synthesis. A practical approach*. Oxford: IRL Press at Oxford University Press. pp 81–100.
Tate WP, Greuer B, Brimacombe R. 1990. Codon recognition in polypeptide chain termination: Site directed crosslinking of termination codon to *Escherichia coli* release factor 2. *Nucleic Acids Res 18*:6537–6544.
Tate WP, Poole ES, Mannering SA. 1996. Hidden infidelities of the translational stop signal. *Prog Nucleic Acids Res Mol Biol 52*:293–335.
Weiss RB, Murphy JP, Gallant JA. 1984. Genetic screen for cloned release factor genes. *J Bacteriol 158*:362–364.
Wilson DS, Szostak JW. 1999. In vitro selection of functional nucleic acids. *Annu Rev Biochem 68*:611–647.
Zhouravleva G, Frolova L, Le Goff X, Le Guellec R, Inge-Vechtomov S, Kisselev L, Philippe M. 1995. Termination of translation in eukaryotes is governed by two interacting polypeptide chain release factors, eRF1 and eRF3. *EMBO J 14*:4065–4072.
Zuker M, Mathews DH, Turner DH. 1999. Algorithms and thermodynamics for RNA secondary structure prediction: A practical guide. In: Barciszewski J, Clark BFC, eds., *RNA biochemistry and biotechnology*. Dordrecht, Netherlands: Kluwer Academic Publishers. pp 11–43.